InSAR and Surveying Evaluation for the Chino Basin

Prepared for Wildermuth Environmental

February 2009

Prepared by: Neva Ridge Technologies
6685 Gunpark Drive
Boulder, Colorado 80301
(303) 443-9966

Contact: David Cohen, Ph.D.
(303) 531-2802
cohen@nevaridge.com

Table of Contents

1. Introduction and Executive Summary

The objective of the work described here is to characterize errors associated with the two main survey types, as implemented in the Chino basin area. It has been recognized that the availability of accurate ground position (vertical and horizontal) measurements over time is important to characterizing the state and health of the basin and to identifying potential problems due to ground motion. Two techniques that are presently employed in the measurement of ground position changes are leveling surveys and differential interferometric SAR (InSAR) surveys. These two techniques, while greatly different in implementation, measure principally the same quantities. Leveling has its roots in the 1800's and earlier but has evolved greatly to the present, taking advantage of precision materials, microprocessor technology and computer processing. The technique has well-established standards and practices, with an associated large literature and body of knowledge. Surveying now comprises a 4-year degree program at many universities. Differential InSAR technology is, by comparison, somewhat new. The study of InSAR began in the second half of the last century when it was recognized that an evolving imaging methodology called synthetic aperture radar (SAR) was potentially capable of producing sensitive measurements of ground displacements. In the intervening 30 or so years, great progress has been made in the corresponding processing technologies.

Both together and separately, these measurement technologies have provided useful information in the management of the Chino basin. While the fundamental measurement products of the two techniques are the same, there are obvious differences in the technologies and advantages and limitations associated with aspects of each. Obviously, a key element of this comparison is the relative accuracies of the two techniques – the subject of most of this repost. Additionally, we can characterize the techniques in terms of the effective temporal and spatial scales available. In terms of spatial scales, where the surface is amenable to InSAR technology, measurements are acquired on a 2D grid roughly every 150 ft. Where the environment is not amenable to InSAR technology (due to the presence of vegetation), measurements are difficult or impossible. In many of the InSAR displacement maps produced thus far, "no-data" regions can be seen – especially to the south of Ayala Park in the agricultural areas. On the other hand, surveying techniques provide measurements on a sparser grid, but a well-designed survey is not generally hampered by the presence of vegetation. In the Chino basin survey, bench marks are spaced by roughly 1000 ft along main roads. For reference, the main Chino subsidence feature is covered by 142 bench marks while the InSAR technique provides about 8000 measurements over the same area. In addition, InSAR data have provided measurement across the entire basin.

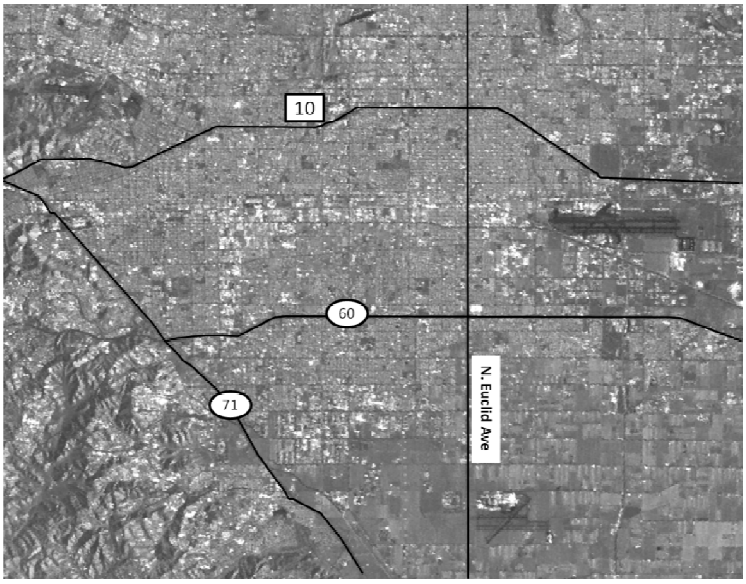

Figure 1: SAR image of area of interest.

From the standpoint of the temporal aspect of the data collections, there are no fundamental limitations to times during which surveying may be performed other than weather. A typical leveling survey is performed over the period of one to two weeks and it is preferable to have no significant precipitation during that period. On the other hand, temporal constraints in InSAR acquisitions are driven by the

predetermined orbit of the satellite. For the systems we have considered, data may be acquired about once per month. Further, since the satellite serves many users, there is occasional competition for the system resources and requested acquisitions are not made. For the frame that includes Chino, requested acquisitions have been unavailable roughly 20% of the time.

A limitation of the InSAR approach, as it is conventionally applied, is that it does not uniquely measure the vertical and horizontal components of ground motion. Instead, it provides the measurement of motion along the line from the satellite to the ground (the line-of-site). For the data processed to date for Chino, the line-of-site is at an angle of about 24 degrees relative to the local perpendicular. This means that we are measuring predominantly vertical motion; we are about twice as sensitive to the vertical component as the horizontal component. In this report we parameterize the error in the inferred vertical measurement in the presence of unaccounted horizontal motion. We also derive the error in the inferred vertical measurement assuming that no horizontal motion is present.

In the current study we present uncertainties in both InSAR and surveying approaches. There are a variety of parameters that impact both of these techniques. For InSAR, the important parameters from the standpoint of accuracy are atmospheric conditions, the presence of ground vegetation, as well as the geometry of the satellite location during each particular pass. While we have no fundamental control of any of these parameters, we *do* have the ability to design the data acquisition and to select data for subsequent processing such that we minimize their impacts. For surveying, in both the vertical and horizontal cases, measurement uncertainties are dependent on the fundamental design of the survey, calibration of the instruments, basic practices, and the presence of extreme weather conditions. Once again, the error sources are not entirely controllable and, while the survey of interest adheres to First Order specifications, this designation does not correspond to accuracy of individual measurements. The basic driver in understanding the accuracies of both InSAR and surveying is that there is no adequate physical model for the error sources for any particular set of measurements. That is, while we can describe the physics of, e.g., how diffraction effects due to atmospheric moisture impact both techniques, there are no independent and coincident atmospheric measurements from which to compute the corresponding errors. The same limitation applies to the presence of vegetation, deviations from accepted practices, etc. As a result, we approach this study by exploiting the fact that considerable data, both survey and InSAR, have been acquired in the Chino Basin. We take advantage of these data in order to extract the accuracies of these techniques. The significance of this approach is that we are presenting the results for actual measurements and for the particular area of interest.

The basic approach is different for each data source. In the case of surveying, the industry standard software that is used to process the raw measurements produces a statistical measure of the quality of each of final bench mark locations. These standard deviations are compiled, for vertical and horizontal cases, to describe the performance of the technique. In the case of InSAR, we take advantage of historical InSAR measurements. Using displacement measurements acquired over short time periods we compute the statistics of deviations from the ideal case of no motion. That is, since very little motion should be present during the short time separations, deviations from zero motion are attributed to error sources. We summarize results in the following table, reproduced here from the final section. Along with the results of the error analysis, we have included comments regarding advantages and limitations of each technique for vertical and horizontal surveys. Details are provided in the remainder of the report. Note that cost has not been included as a factor in any of the analyses presented here.

Comments	Error Analysis
VERTICAL	
The most common interpretation of the InSAR measurement is that it corresponds primarily to vertical motion. Under this assumption, we compiled data from 16 separate measurements over a common area (just NW of the main Chino subsidence feature). Based on roughly 15,000 pixels, we produced statistics for the error. • InSAR produces measurements (with the statistics quoted to the right) on a grid of roughly 150 feet. With newer satellite systems, this spacing may be improved. • Many 10's of square miles may be covered by a single data set – at intervals of roughly one month. • The conventional InSAR approach produces displacement measurements along the satellite line-of-site. These may be resolved to 2 dimensions using a priori knowledge. For data processed to date, sensitivity to vertical motion is 2x sensitivity to the horizontal component. • More advanced techniques may produce 2 dimensions of motion based on the data itself.	90% of the 2σ error values are 0.77 cm (0.025 ft) or less. Opposite-side-InSAR: 90% of the 2σ error values are 0.54 cm (0.018 ft) or less.
The industry standard STAR*LEV software produces statistics for each bench mark. These 1-sigma values are converted to 2-sigma (assuming Gaussian statistics). • The current Chino survey produces measurements at separations of roughly 1200 to 2500 feet over the extent of the main subsidence feature, with the Ayala Park extensometer used as reference. • Leveling provides explicit vertical measurements, independent of horizontal component. • Larger areas can be surveyed, although distance from Ayala Park extensometer results in measurement noise.	90% of the 2σ error values are 1.42 cm (0.047 ft) or less.
HORIZONTAL	
As discussed above, conventional InSAR produces line-of-site displacements. We may assume horizontal-only motion (which is likely not of interest here), have *a priori* knowledge of vertical motion, or use the opposite side InSAR (OSI) approach to estimate the horizontal component. • Horizontal motion is not a typical direct output of conventional InSAR technique. Although, it can be done with *a priori* knowledge of vertical motion. • Opposite-side-InSAR (OSI) can produce separate horizontal/vertical components; requires twice the data. This technique has been demonstrated in a limited way. (Note that there is an excellent candidate Chino data set for this demonstration for 2008.)	Horizontal-only or *a priori* vertical: 90% of the 2σ error values are 1.73 cm (0.057 ft) or less. Opposite-side-InSAR: 90% of the 2-sigma error values are 1.22 cm (0.040 ft) or less.
The industry standard STAR*NET software provides standard errors computed based on the equipment characteristics and the geometry of the horizontal network. Since this survey is designed for easting strength only, only these values are analyzed. However, it is important to note that motion of the reference points, to the extent that it is present, will further degrade these values. • Predicted errors for horizontal difference survey are good but don't account for possible motion of reference points. • Survey is designed for superior strength in easting. • More stable horizontal control would improve results.	Easting 2σ error values are 1.10 cm (0.036 ft) or larger. Insufficient northing strength to estimate errors.

In evaluating the differing modalities for measuring and monitoring ground motion in the Chino Valley, there are a variety of *dimensions* to the problem. We mean by this not only the spatial dimensions of the measurements, although these are significant considerations. The evaluation must take into account spatial coverage, temporal coverage, and the accuracy of the candidate measurement methods. The table above points to a variety of differences between the methods.

For the current approach to monitoring ground motion in the basin, a significant limitation is a lack of precise knowledge regarding the horizontal component of motion. For the two measurement techniques, horizontal motion is either not separable (conventional InSAR) or there is insufficient information to describe its accuracy (surveying). As pointed out in the table, the approach to uniquely extracting the horizontal component from InSAR (OSI) is very promising but not fully demonstrated. We return to OSI shortly. As for the horizontal survey, it is a well-demonstrated technique but, in this case, is not designed to fully exploit its potential. In particular, no horizontal control has been used so that difference measurements are impacted by the unknown horizontal motion of the reference points. Clearly, improved and better characterized measurements will require use of horizontal control in the area. There are two conceivable improvements to this network that may address this issue. The first is the possible use of existing horizontal control. Unfortunately, despite the existence of a large number of monuments in southern California, maintained by the NSF Plate Boundary Observatory (PBO), and the National Geodetic Survey's (NGS) continuously operating reference (COR) locations, only a single monument is in the vicinity of the region of interest. However, this is located approximately 2.8 miles from the Ayala Park extensometer.

On the other hand, a possible approach is to improve the horizontal survey by maintaining horizontal control using a GPS survey. Note that, while GPS is in principal a solution for the entire ground motion monitoring problem in the Chino area, in reality it will be severely limited by the presence of trees (obscuration of satellites) and power lines (interference and multipath). For these reasons, and based on discussions with Jim Elliott, a full GPS solution is not likely to be technically feasible. However a partial GPS solution remains feasible. A notional approach would be to use a network similar to that in Figure 15 with the end points of each horizontal leg provided by GPS coordinates obtained using survey grade GPS procedures and equipment. Such an approach should provide control for each leg with an accuracy of better than 1 cm, depending on the fidelity of the equipment and procedures. If it is desired, such a network could be expanded to provide improved strength in the north-south direction. Note again that no consideration of cost has been factored in to this analysis.

Finally, we return to the option of performing opposite side InSAR (OSI) at this site. Previous analysis (not for the Chino area) has been primarily limited by atmospheric interference. Our analysis presented above suggests a 2-sigma accuracy of 1.22 cm (easting) and 0.54 cm (vertical) or better. The procedure is sound and the main question regards whether the expected motion is sufficient to bring the horizontal signal above the noise. The basic approach of the publication referenced above is applicable in the general analysis of the data. In fact, the quality of the recent SAR data in the Chino area – for the period 2008 – is excellent and data have been acquired in both ascending and descending orbits. These data, not all of which have been purchased, exhibit excellent baselines for both ascending and descending passes. As a result, there is a good opportunity to demonstrate this technique assuming that there is sufficient motion during this period to provide a quality measurement above the noise. Based on the predicted noise levels, this would require a horizontal component on the order of 2 cm for this time period.

The current line-of-site InSAR approach to monitoring in the Chino basin area provides a high sensitivity to motion and, through the temporally dense data being acquired, sensitivity to its onset and time dependence. Although the conventional InSAR approach does not provide unique horizontal and vertical components, it certainly provides a measure of the magnitude of the motion to better than one centimeter.

Collection of high quality data, with good baselines, has been very reliable for this frame. An excellent set of data, being processed as this report is being written, has been collected for 2008. The InSAR approach currently being pursued, in which many data acquisitions are being made and a dense subset is purchased, appears to be a very promising approach to capturing the dynamics of ground motion during the year. Furthermore, to the extent that the horizontal survey uses reference points that are well removed from the known subsidence regions, the technique should, based on the results below, provide measurements that are within about one centimeter. While a temporally dense set of data is usually preferable to a sparse one, the horizontal survey data can provide a pair of ground motion reference points for the InSAR survey, at spring and fall intervals. This continues to be valuable, especially in the case that significant motion is detected in the InSAR results. In that case, it should allow for separation of horizontal and vertical components, for the spring and fall measurements. According to the results here, more frequent horizontal surveys would provide additional insight into the horizontal/vertical motion components, but not necessarily any new information regarding the magnitude of motion or its onset.

2. Interferometry Overview and Error Sources

The launch of several international civil synthetic aperture radar (SAR) missions during the past 17 years has provided valuable new data sources for detecting a variety of phenomena on the Earth's surface. The coherent nature of the basic technology allows sensitive measurements over large areas not possible with other sensors. Such measurements include height, height change, and change in the properties of the scattering surface over time. For the satellites considered in the present work, the satellite orbits the earth once every 100 minutes or so in a very nearly north-south orbit. The radar antenna illuminates the ground in a swath off to the side of the direction of travel (Figure 2). The system emits on the order of 1500 pulses each second and listens for the portion of the radiation that is scattered back to the antenna. This information is recorded and retransmitted to an Earth receiving station for later processing. In the approach of specific interest here, the SAR satellite views the same region at two different times and from roughly the same position in space. The basic product created is a SAR image corresponding to each of the collection times. A sample image is shown in Figure 2. This image is a radar intensity image and contains information regarding terrain properties and man-made structures and their tendency to reflect radar energy back to the satellite. Many man-made features and rough surfaces (such as agricultural areas) tend to be very effective "backscatterers" at radar frequencies; these areas appear bright in the radar image. Surfaces that are smooth on the scale of a radar wavelength (5.6 cm in this case) tend to act as mirrors so that incident radar energy bounces away from the satellite. Such surfaces include quiet water surfaces as well as runways and paved roads.

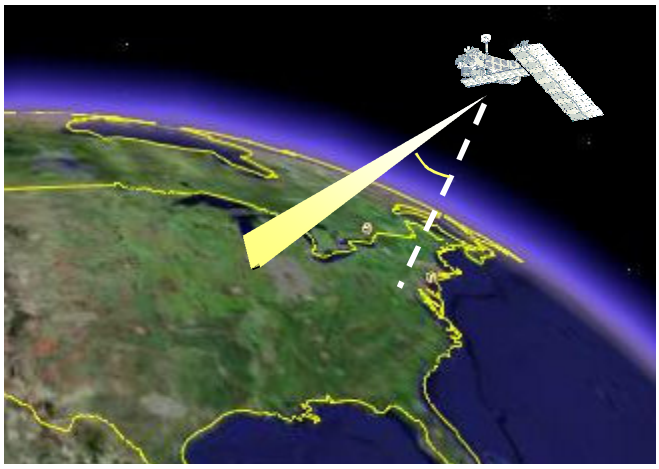

Figure 2: SAR satellite imaging diagram.

An important characteristic of the SAR data acquisition process is that the phase of the radar signal is known when the energy is recorded and when the scattered energy is received. As a result, it is possible to exploit the sensitivity of this phase measurement to various phenomena. In particular, we are interested in the ability to use small phase variations in the processed data to determine motion on the surface of the earth. The general technique is called SAR interferometry (InSAR) and the application to ground deformation measurement is often termed differential InSAR (DifSAR). In the current document, we use InSAR as the generic term for the processing we do. For conventional InSAR processing the primary output is the change in the path length to each point on the ground, as seen from the satellite, and over the two times of data acquisition (typically weeks to months). This *line* connecting the satellite and the grond is typically called the line-of-site (LOS) and, for the satellites considered here, is oriented at 24 degrees from the local perpendicular to the ground surface. Figure 3 shows the basic configuration. The line-of-site is oriented at 24 degree from the local perpendicular and is rotated in the plane of the earth's surface by an angle of about 8 degrees. In general, the basic InSAR technique cannot distinguish horizontal motion from vertical motion. For a given InSAR displacement measurement d_t along the LOS, the actual horizontal and vertical displacements d_v and d_h, for the geometry in the figure below, may be any pair of values that satisfy the equation.

$$d_t = d_v \cos(24) + d_h \sin(24) \qquad (1)$$

Given this horizontal/vertical ambiguity, it is typical in many InSAR surveys that an assumption is made that all motion present is vertical (setting d_h to zero in the above equation) so that the vertical motion can

be directly computed. In other cases, the line-of-site measurement is reported without an attempt to remove the ambiguity. Likewise, in the case that measured motion is known, or suspected to be, entirely horizontal, one can convert from the total displacement to the horizontal displacement by setting the vertical term to zero. In the analysis to follow, we will assume that the LOS measurements are dominated by the vertical contribution and derive the errors. Then, in a following section, we will further discuss the implications of the vertical/horizontal ambiguity and provide a quantitative analysis and suggestion for partial removal of the ambiguity.

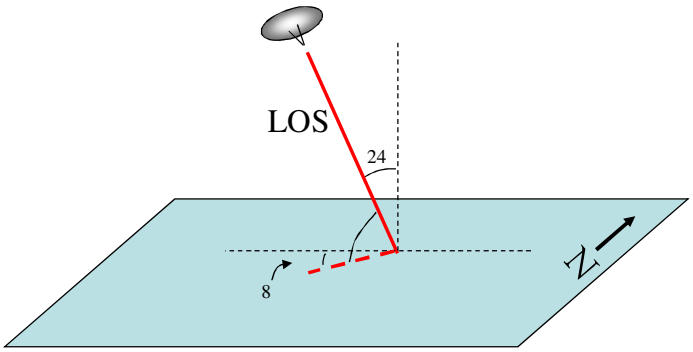

Figure 3: Basic radar configuring showing the line-of-site (LOS) and relevant angles.

2.1. InSAR Noise Contributions

There are several good treatments of the contributions of various sources to errors in SAR interferometry. A canonical source of this is Rodriguez[1], a relatively early paper that nevertheless provides a good background of the theoretical error sources in SAR interferometry. The theoretical error sources traditionally considered in conventional interferometry are generally allocated to two areas. These are geometry and environment. In the case of geometry, to the extent that there is uncertainty of the geometry of the data acquisitions, there will be corresponding uncertainty in the interpretation of the resulting interferometric phase. For example, since the performance of any interferometer depends critically on knowledge of the separation between the elements of that interferometer, it is critical that this information is known accurately. While these measurements are performed using instrumentation on-board the satellites, the *raw* results are typically not of sufficient quality for accurate InSAR measurements. However, advanced InSAR processing is capable of adaptively refining the estimates of these geometric parameters so that the effects of uncertainties in these parameters are minimized.

With that said, some of the theoretical error terms do not significantly come into play since they can be corrected with a priori knowledge. What is left is the two dominant error terms in conventional interferometry. These are decorrelation and atmospheric interference. These are discussed in turn below.

2.1.1. Decorrelation Noise

Qualitatively, the coherence between two SAR images comprising an InSAR pair may be thought to represent the degree to which they are similar on the scale of a radar wavelength (a few centimeters.) If a region is largely disturbed during the time between the two InSAR collections, then the resulting measurements will be extremely noisy, as will the height measurements; and the corresponding coherence will be low. The term decorrelation refers to the degradation of coherence. Below we discuss this mechanism in somewhat more detail.

A key to success in InSAR processing is the magnitude of the complex coherence of two SAR images. This quantity is defined by the following:

[1] E. Rodriguez and J.M. Martin, IEE Proceedings-F, Vol. 139, No. 2, April 1992

$$\rho \equiv \left| \frac{\langle S_1 S_2^* \rangle}{\langle S_1 S_1^* \rangle \langle S_2 S_2^* \rangle} \right| \qquad (2)$$

Where $S_{1,2}$ represent the complex SAR images. For perfectly coherent data, is equal to one; it is zero for a complete loss of coherence. This quantity is a measure of the degree of noise present in the interferometric phase measurements; and since the phase carries the information regarding the ground position changes, it is critical to successful InSAR. Physically, it is a measure of the degree to which the scattering center distribution within a resolution cell has changed between the two data acquisitions. Coherence can degrade as a result of a variety of phenomena. These include vegetation, geometric properties of the two data acquisitions, and weather-related and man-caused surface changes. For example, consider a single interferometric pair. In the case that the dominant scatterers in a particular region have been completely "rearranged" by some process such as harvesting of a field, excavation, or simply the change in vegetation that arises with wind, there will be a significantly reduced coherence for this region. Likewise, if the geometries of the two interferometric SAR acquisitions are significantly different, even if the scatterers are unchanged, their phase sum at the two very different locations will differ greatly. This latter effect is known as geometric decorrelation. Finally, there are other contributions to the coherence of a particular area such as the strength of the scatterers as well as the presence of volume scatterers. Regardless of the source of the decorrelation, it is important to recognize that the quantity can be estimated directly from the data, as well as related directly to the expected phase noise level in the associated interferometric measurement.

The image in Figure 4 shows a map of the coherence, for the Chino Valley, for a particular interferometric pair. The coherence scale runs from blue through red to yellow, representing increasing values. The intensity of the colors is determined by the underlying SAR intensity image. Note that low coherence is observed in the agricultural areas to the south as well as in some of the mountainous regions. This caused mainly by vegetation in these areas and, possibly, by radar shadows in the mountains.

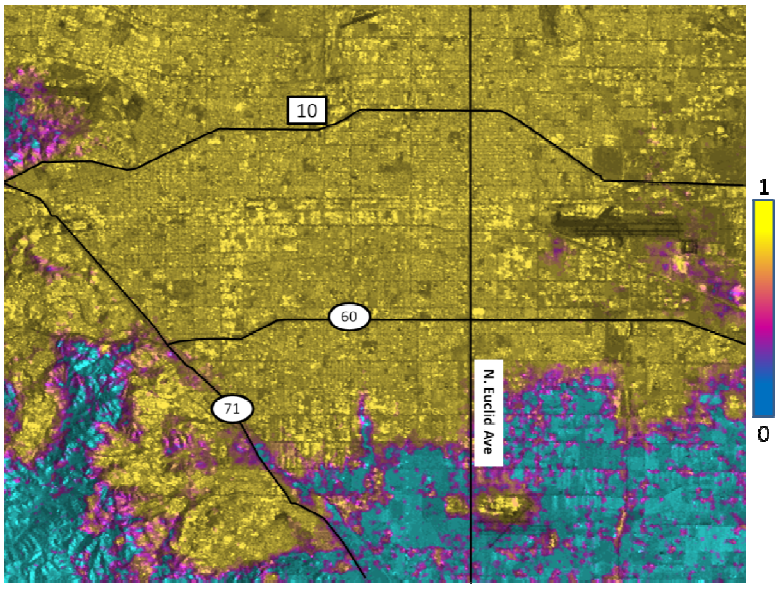

Figure 4: Coherence represented as color and superimposed on a SAR image. This particular interferometric pair contains two images from 1/26/1996 and 4/6/1996. These were acquired by the ERS sensors.

Based on an informed selection of data, it is possible to minimize the effects of decorrelation. This is achieved by choosing data with small temporal and spatial baselines. (In fact, this the principal driver behind the approach of measuring displacements over long times by using many short, contiguous steps.) In addition, the processing approach itself is capable of mitigating much of the decorrelation using an iterative approach to estimate satellite geometry. What is primarily left is the effect of vegetation, weather, and man-caused changes on the ground. The importance of coherence is that it can be shown quantitatively to relate directly to the noise in the height measurements derived from InSAR. The equation below relates coherence ρ to the standard deviation of the InSAR vertical displacement measurement. Here, N is the number of pixels used in the averaging process and C is a constant containing numerical factors and the radar wavelength.

$$\sigma_v = C\sqrt{\frac{\left(1-\rho^2\right)}{2N\rho^2}} \tag{3}$$

Noise due to decorrelation is an important part of the description of the noise in InSAR measurements. In the current analysis, we present a representative result for this quantity from a particular InSAR pair. From this we derive an estimate of its contribution to the measurement noise. The plot in Figure 5 shows the distribution of coherence values for the data presented in Figure 4. Here we see a peak in the highest coherence bin with a steep falloff and a gradual decline. The relatively stable region for smaller values of coherence correspond to the areas in the image with red/blue values.

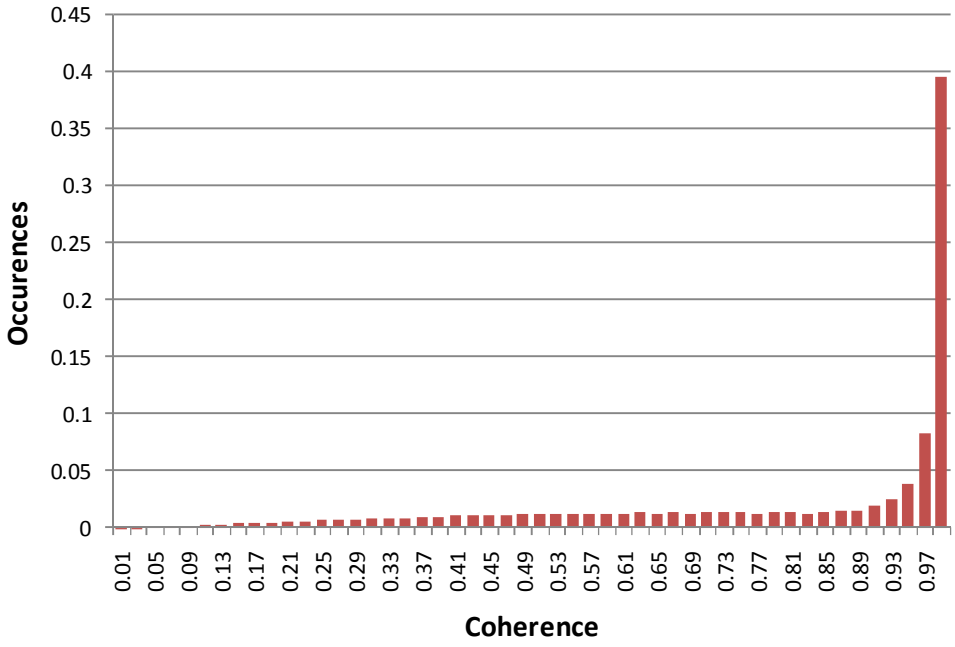

Figure 5: Histogrammed coherence values.

In the coherence discussion, it is important to note the following: In the course of deriving ground displacement from these data sets, it is common to threshold the coherence at 0.70 and mask out regions with lower values. In doing so, we remove areas with noise characteristics that are known to be unacceptably high. For the remaining unmasked data, corresponding to roughly 70% of the full data set in this case, we may apply the relation in equation 3 above and draw the conclusions shown in Table 1 regarding the impact of this measurement noise source. This table shows the computed height standard deviation (based on equation 3) at various percentiles of the pixels in the test image. From this result, we

can see that that 90% of the measurements that are included in the unmasked region have a two-sigma value of 4 mm or less (with most of the values well under this). While this is not a large error source for most of the pixels, it is nevertheless important to understand that the height error sources are varied. In the next section, we consider the atmospheric noise contribution.

Table 1: Conclusions drawn from analysis of coherence contribution to height noise.

Percentile	Vertical Height Standard Dev. (cm)	2x Standard Dev. (cm)
Top 60%	≤ 0.05	≤ 0.10
Next 20%	≤ 0.13	≤ 0.26
Next 10%	≤ 0.20	≤ 0.40
Next 10%	≤ 0.30	≤ 0.60

2.1.2. Atmospheric Noise

The second significant source of error in SAR interferometry is atmospheric interference. Variations in refractive index of the atmosphere due to variations primarily in water vapor content lead to phase delays at radar frequencies. The result is a corresponding phase signature in InSAR imagery that varies with the particular water vapor distribution. Such a phase signature has been known to be indistinguishable from a ground motion signature. Figure 6 shows an example of particularly severe atmospheric interference in a 3 month interferometric pair in the southwestern US. Here we see on the order of one full cycle of interferometric phase (2π radians) varying locally. This extreme example corresponds to an apparent variation in surface displacement of roughly 3 cm or more. That is, if the InSAR phase signals in the image below are interpreted as displacement signatures, the error is fairly dramatic. This situation means that great care is required in the processing, combination, and interpretation of InSAR data. A significant advantage in acquiring more frequent SAR collections is that those with anomalously large atmospheric interference may be omitted from the processing stream.

The effects of atmospheric interference in SAR imagery may be at least partially mitigated via a few possible approaches. Not all of these are discussed here, nor are they necessarily commonly applied. However, a robust approach that *is* employed commonly, including during the Chino work, is temporal stacking. This is, in many cases, a very effective technique for producing atmosphere-mitigated results based on a series of SAR acquisitions. As discussed in the previous subsection, the approach of combining consecutive InSAR displacement measurements is desirable since it makes use of minimal temporal baselines and thereby minimizes temporal decorrelation. However, a second advantageous feature of this approach is that, despite the fact that several images are being combined, the atmospheric interference in the final product contains contributions from only the first and last image. The reason for this is straightforward. Consider the processing of three data acquisitions (a, b, and c) that are acquired at three consecutive times. The InSAR displacement map created from the first two images contains the displacement of ‘b’ relative to ‘a’. The second displacement map contains the displacement of ‘c’ relative to ‘b’. Now consider an atmospheric disturbance occurring in ‘b’ that results in a phase delay and a corresponding apparent ground motion in the (a-b) InSAR result. In the (b-c) InSAR result, the same disturbance is present, but it is of the opposite sign. As a result, when we “stack” this temporal series (i.e., when we sum the (a-b) displacement with the (b-c) displacement) the atmospheric contribution of ‘b’ will cancel to leave only the contributions of ‘a’ and ‘c’. There are two distinct points that arise from this discussion. First, the technique of stacking – the summation of consecutive short time displacement measurements – does not result in a constructive accumulation of atmospheric interference. This is despite the fact that a, say, increasing subsidence feature *will* add constructively with this technique. The second point is that, given multiple SAR acquisitions over a given time period, an optimal stacking set

can be identified so as to minimize the atmospheric interference. This is achieved by using starting/ending SAR frames with minimal atmospheric interference.

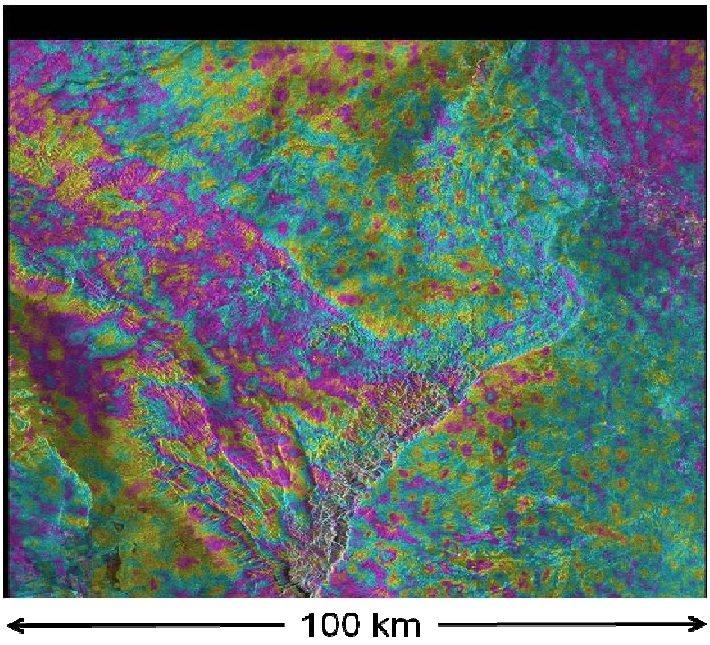

Figure 6: Example of atmospheric interference in an InSAR phase image. One color cycle represents 2.8 cm of apparent motion.

The net result is that, while the stacking approach allows for the accumulation of displacement signals over a long period, it results in atmospheric signals that correspond to only a single pair of images. In addition, according to the discussion in the previous section, stacking requires shorter time steps (temporal baselines) for each constituent InSAR pair, resulting in less decorrelation due to temporal changes on the surface. The figure below (Figure 7) shows two displacement measurements from the ERS Chino dataset from the 1990's. These are scaled per the color bars on the right of each image to show the vertical measurement in the Chino area for two short-time pairs. It is important to note that these images are scaled so as to emphasize small displacements; these scales are roughly three to four times more sensitive to motion than those typically displayed, which have a range around 5 cm. The dates corresponding to these pairs are 10/23/1999-11/27/1999 and 2/5/2000-4/14/2000. The first of the pairs shows a rather representative displacement measurement for this data set while the second is considered extreme in terms of atmospheric interference. These were chosen with short temporal baselines in order to minimize the contribution of actual ground motion to the result. However, in the upper image note that there are apparent ground motion signatures corresponding to locations of know historical motion. The first is south of highway 60 and north of highway 71, corresponding to the location of the main historical subsidence feature. This result represents a few millimeters of subsidence during this 35 day period. Also, in the same image a small region of uplift is seen that is possibly associated with the San Jose fault. These two features are very possibly real, although there is no independent verification of this. Otherwise, one observes a slowly varying apparent displacement signal that seems to not correspond to known regions of historical subsidence. This component has an amplitude range of roughly -0.7 to +0.5 cm for this particular image. In the second image below, the situation is somewhat more severe. The range of values is slightly more broad (-0.75 to +0.75) and the interference is more present in this data set. Once again though, this second image corresponds to one of the more severe cases for this region from the standpoint

of atmospheric interference. In this image, as well as the previous one, some distinct interference can be seen in the Chino Hills to the west. Such observations are not entirely uncommon since mountainous regions interact with the atmosphere differently than valleys.

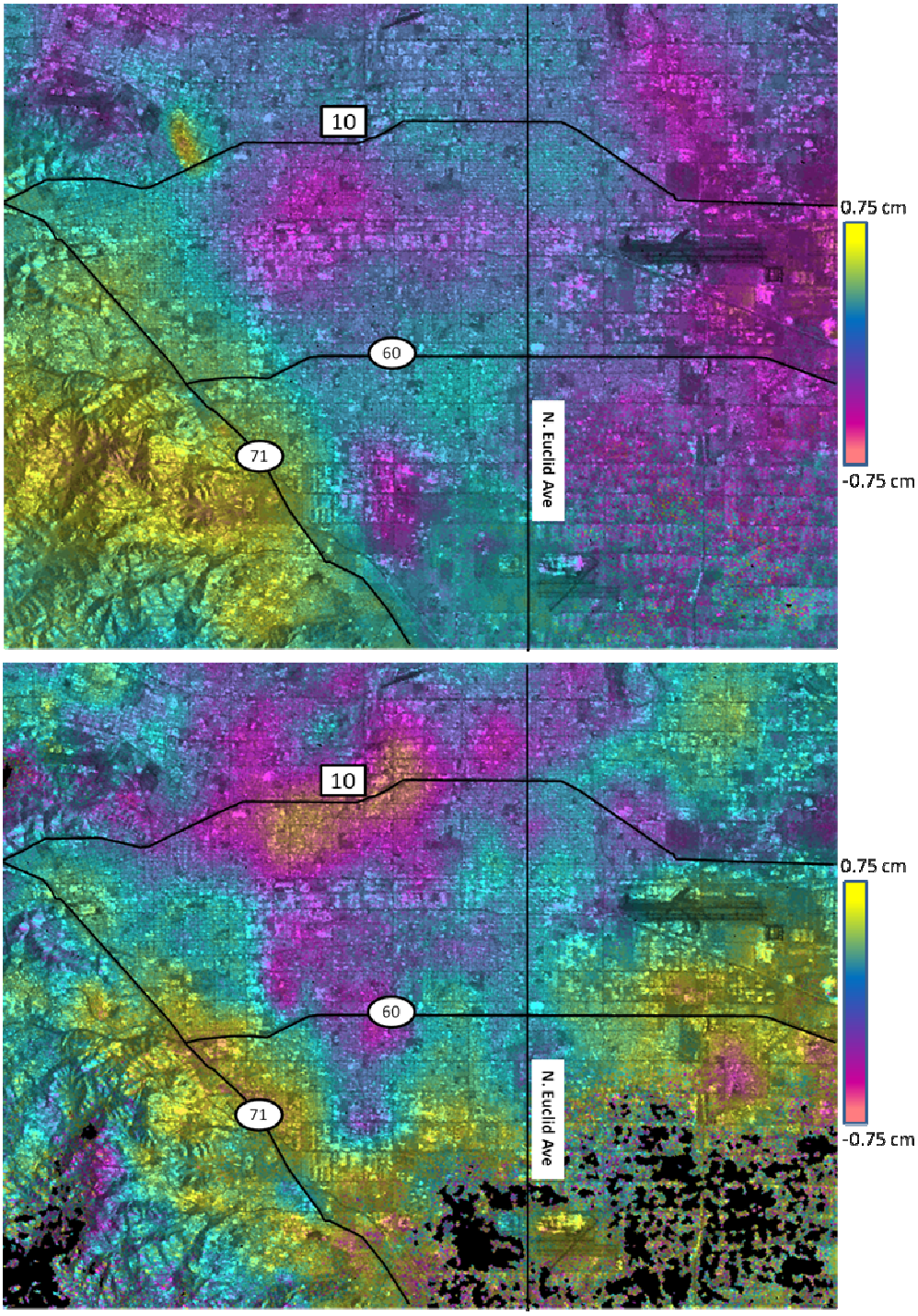

Figure 7: Sample vertical displacement measurements from two sets of InSAR data. It is important to note that this scale is exaggerated compared to the more conventional scale in which one color cycle represents 5 centimeters.

The information we can extract from this analysis is *qualitatively* useful in the sense that it provides the range of atmospheric interference expected for this data set. We can conduct a more thorough analysis using a larger group of InSAR measurements for this site. In the following section, we perform a quantitative analysis of the measured InSAR displacement errors for the Chino area.

2.2. Quantitative Evaluation of Line-of-Site Displacement Errors

The discussions above regarding the dominant sources of InSAR displacement errors provide a semi-quantitative or qualitative description. We see that the effect of decorrelation is to introduce a random error from pixel to pixel; for a given pair, we can characterize the expected value of this error. On the other hand, we see from InSAR data that atmospheric effects are visually apparent depending on the particular pair. There is no useful model for predicting the atmospheric contribution to the displacement error. This is because the prediction would be highly location-dependent and would require detailed 3-dimensional atmospheric measurements corresponding exactly to time of data collection. As a result, we employ an empirical approach to describing these errors, taking advantage of the relatively large number of SAR images that have been obtained for the Chino site. In lieu of actual models, this approach has the advantage of quantifying results for the particular area of interest. Since atmospheric effects (based on the presence and variability atmospheric moisture) vary geographically, this approach gives the best statistical understanding of the behavior of total InSAR noise for the Chino basin area.

For the historical data set comprised of ERS acquisitions from the 1990's, we have isolated the 16 interferometric pairs with spatial baselines less than 400 meters and temporal separations of less than three months. In this way we minimize the contributions of both temporal decorrelation and actual ground motion, and isolate the atmospheric contribution. The approach here is to compute the phase variation within a region of interest and determine the statistics of the combination of many such measurements. This gives us a quantitative evaluation of the expected phase deviation for the Chino area specifically. The following table shows the InSAR pairs used in this analysis. These comprise all of the short spatial and temporal baseline pairs from the previously obtained ERS 1 and 2 data for the Chino area.

Table 2: InSAR pairs used in the statistical analysis of the Chino area.

	InSAR Pair (yyyymmdd)	Spatial Baseline (m)	Separation (days)
1	19920826-19920930	240.5596	35
2	19950421-19950526	28.1069	35
3	19960126-19960406	-194.8633	71
4	19970111-19970215	-303.3259	35
5	19970215-19970426	-158.3095	70
6	19970426-19970531	87.7861	35
7	19970426-19970705	172.6706	70
8	19970531-19970705	84.8845	35
9	19970705-19970913	283.4039	70
10	19970913-19971018	88.888	35
11	19980131-19980411	-193.9999	70
12	19991023-19991127	-171.285	35
13	19991127-20000205	3.4498	70
14	20000205-20000311	-193.2922	35
15	20000205-20000415	51.2043	70
16	20000311-20000415	244.4965	35

The analysis of these data sets proceeds by identifying a common region within each image in which InSAR displacements are to be characterized. Given all 16 pairs in the above table, we then accumulated the entirety of these measurements to determine the statistics of the resulting distribution. There were a few considerations when selecting the location for the measurement region. Clearly, we would like this region to be in the vicinity of the actual area of interest since atmospheric activity is clearly dependent on the geographic location (and the proximity to mountains, water, etc.). It is desirable to avoid the mountains in this region since, as we have seen above, the locations often result in anomalous atmospheric contributions. (In addition, no mountains are of interest in the Chino work.) One choice for the measurement region is that corresponding to the main historical Chino subsidence feature, which is roughly south of Mission Blvd. and west of Mountain Ave., since this is a prime area of interest. However, during the 1990's, the period during which these data were acquired, and even for the short temporal separations indicated in Table 2, a few of the displacement maps contain clear subsidence signals in the region of the known historical feature. Any real ground motion occurring in the area of interest will skew the results. Instead, we have chosen a test region in the Chino Valley for which historical subsidence is minimal. That region is shown in the rectangular outline of Figure 8. The area of this measurement region is approximately 18 square miles.

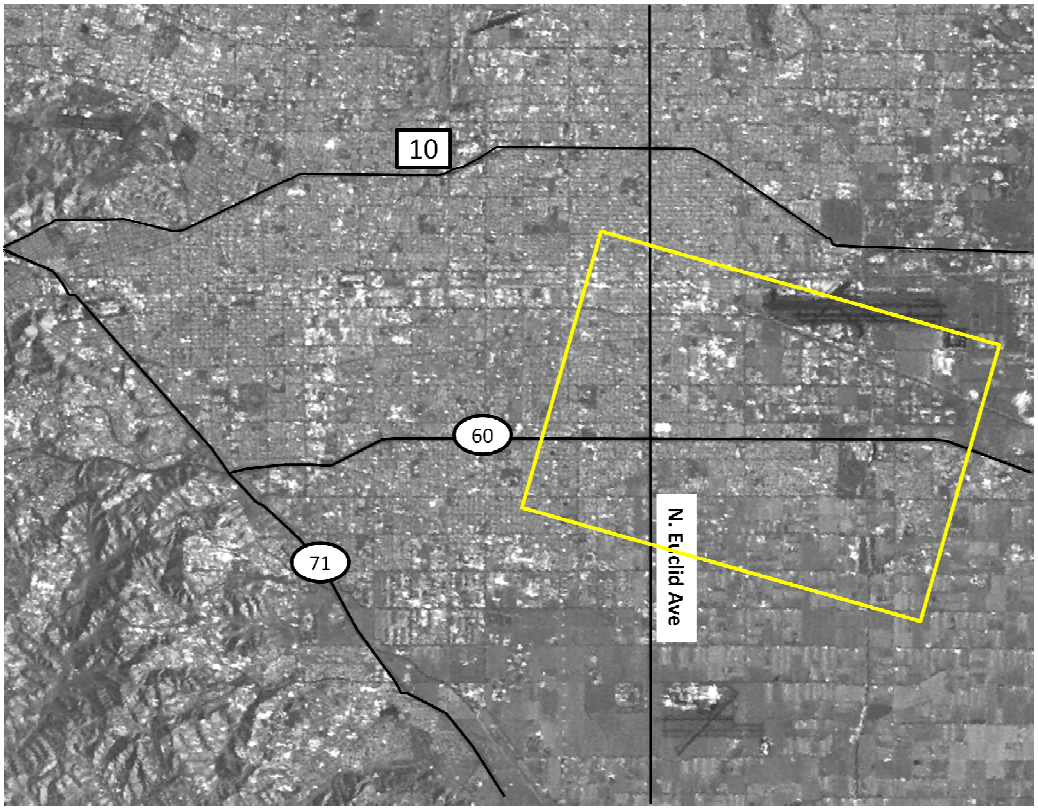

Figure 8: SAR image of Chino Basin region showing area used for atmospheric error analysis.

For each InSAR displacement map, we computed the mean displacement within a 9x9 reference patch located at the center of the box and subtracted that value from all measurements. Next, the values of the resulting displacements were accumulated. The results of this measurement are shown in Figure 9 below. Here, the accumulated histogram of the displacement values within the box in Figure 8, and for all of the 16 InSAR pairs is represented by the solid squares. Note that the vertical scale is in arbitrary units. In the same plot, the solid curve is the best fit (least-squares) of a Gaussian function to the measured data. Since the atmospheric signal is random from time to time (the atmosphere is not correlated over a 35 day

period), the assumption that the resulting displacement measurements will be distributed according to a Gaussian appears to be approximately valid. The small deviation of this result from this functional form is likely due to the fact that some actual ground displacements were present in the measurement box in Figure 8. The statistics for this distribution are shown in the same figure. The non-zero mean value of 0.05 cm is consistent with the presence of a small subsidence signal in some of the measurements. These results of this data analysis show a 2-sigma deviation (95%) of the measured values to be just under one half of a centimeter.

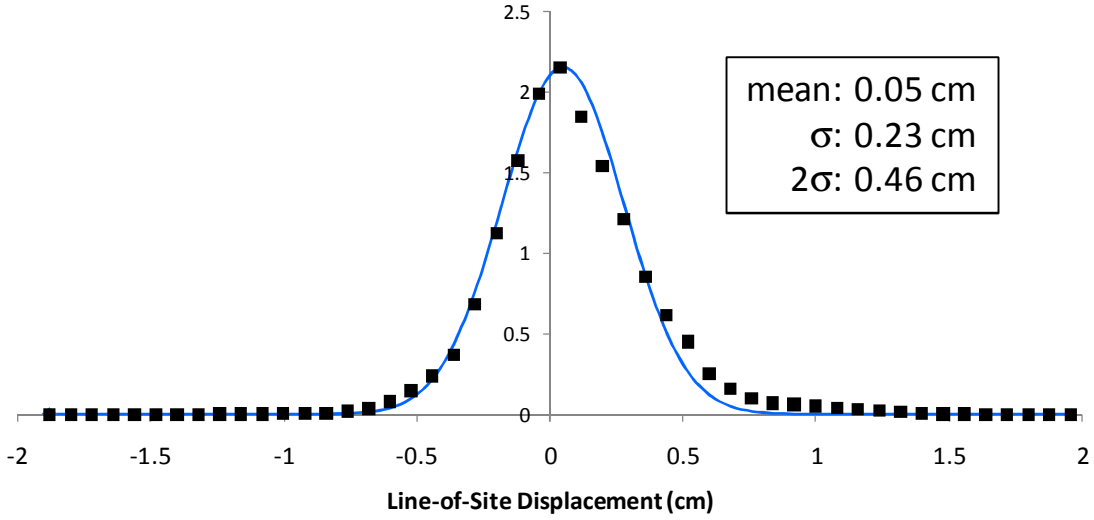

Figure 9: The measured histogram of InSAR displacement measurements within measurement box (arbitrary vertical scale) is shown as solid squares. The curve is the best (least-squares) fit to a Gaussian.

A further, possibly more conservative analysis of the data can provide the expectation values for individual InSAR measurements. While the above plot rigorously captures the statistics of the collection of all 16 displacement measurements, it does not capture the statistics of individual InSAR measurements. In other words, if we were performing several measurements simultaneously, the above distribution would be a good estimate (based on a sample) of the result. What it does not capture completely is the distribution of mean values among the 16 measurements. The mean values occur due to local variations in the atmospheric interference that are not removed with the reference patch. Since the actual measurement we are trying to characterize is a single measurement of the InSAR displacement, we should include the statistics of the mean displacement of the individual measurements in our analysis. Table 3 contains the values of the mean displacement and standard deviation for *each* of the 16 displacement measurements.

Table 3: Derived values for the 16 InSAR displacement measurements.

	Measured Mean (cm)	Measured Standard Dev. (cm)
1	0.42	0.45
2	0.22	0.27
3	0.08	0.33
4	-0.07	0.17
5	0.10	0.20
6	0.22	0.18
7	0.07	0.23
8	-0.18	0.27
9	-0.04	0.32
10	0.15	0.22
11	0.15	0.22
12	-0.05	0.12
13	-0.14	0.16
14	0.03	0.17
15	0.20	0.26
16	0.15	0.23

If we first consider the average value of the standard deviation, the result is 0.237 cm, consistent with the one-sigma value determined above. However, if we next consider the standard deviation of the measured mean values, the

result is 0.154 cm. This leads us to the conclusion that, within a single InSAR measurement, the contribution of the local bias might be significant. As a result, we can compute the deviation of the distribution, for each of the 16 measurements, relative to zero. This is because, under our assumption, the short-time InSAR measurements should contain no displacement signal other than atmosphere and noise contributions. We are therefore calculating the deviation of the measurements relative to the expected value, which is zero. The result for the InSAR data set is seen in the following graph. Here, we have plotted the distribution of standard deviations for the 16 InSAR samples used in this analysis. For this data the mean value is 0.29 cm, with 90% of the values less than or equal to about 0.35 cm. In order to produce a conservative estimate, we have repeated the analysis to produce the 2-sigma displacement measurements and the result is that 90% of the 2-sigma InSAR displacement values are less than 0.70 cm. Again, note that this more conservative analysis produces an uncertainty that is larger than that shown in Figure 9. Since these represent measurements along the line-of-site, we can convert to vertical displacement using equation 1, under the assumption that there is no horizontal motion component. The result is an estimated vertical uncertainty of 0.77 cm.

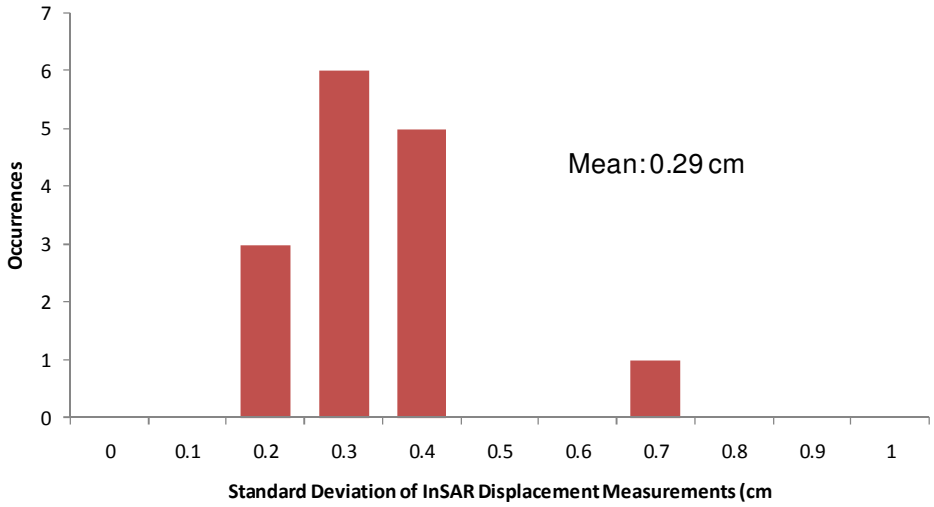

Figure 10: The distribution of computed deviations, for each of the 16 InSAR measurements, relative to zero mean. Note that the mean value of these quantities is 0.29 cm.

Finally, it is important to note that, in Table 3**Error! Reference source not found.**, the first entry contains somewhat anomalous values of both mean and standard deviation values. In fact, the InSAR results corresponding to this measurement show considerable noise in the measurements that would lead to erroneous conclusions regarding the presence of ground motion in the area. The practice in cases such as this is to simply disregard the particular data set. This is a typical triage step in the processing of displacement data and performed following a visual inspection of the data. As in any measurement approach, occasional measurements do not meet the specifications of the process, due to hardware, software, human, or environmental errors that are simply outside the bounds of the expected performance. Unfortunately, in the case of InSAR, it is often not feasible to obtain a new measurement since we are limited by the orbit of the satellite. Given a sufficiently dense data archive, however, it is often feasible to replace the data set with one with more benign atmospheric effects and acquired at a nearby time.

2.3. Vertical and Horizontal Components

Earlier in this section we briefly discussed the interpretation of the InSAR motion measurements in the context of vertical and horizontal components. The conclusion there was that we are measuring motion only along a single vector and that there is no unambiguous way to uniquely determine the actual motion

in three dimensions from a single (InSAR) measurement. In most applications it is the vertical component that is dominant and primarily of interest. In other applications, it is the existence of motion, as measured along the line-of-site, that is of interest. The fact that SAR systems of interest here have an incidence angle that is steep (24 degrees in Figure 3) means that the InSAR measurement is most sensitive to the vertical component of motion. However, the horizontal component does contribute to the measurement and should at least be considered in the analysis.

In the following section, we will modify the results of the previous analysis based on the assumption that the net displacement measured is solely due to vertical displacement; this will slightly increase the value stated in the previous section. Following that, we will briefly quantify an additional source of uncertainty in the InSAR measurement associated with the (false) assumption of vertical motion only. In the section following that, we will describe an approach to measuring two dimensions of motion using InSAR data collected from opposite directions.

2.3.1. Vertical Motion-Only Results

Given the assumption that all of the measured motion is due only to vertical motion, we can use equation 1 to compute the inferred vertical motion from the net motion. Likewise, our error bounds computed above for the net displacement will have to be modified according to the same equation and will be scaled by the inverse of the cosine of the incidence angle. As a result, we find that, for vertical motion only, 90% of the 2-sigma error values are less than 0.77 cm.

2.3.2. Impact of Horizontal Motion in Conventional Approach

As discussed above, most of the InSAR displacement measurements provided for the Chino basin, as well as to other customers contain either the assumption that the actual motion is in the vertical direction, or no assumption regarding the actual motion. In the former case, measurements are back-projected into the vertical direction (following Equation 1) while, in the latter case, the full measurement along the line-of-site is produced. Clearly, while this covers most cases of interest, it certainly does not cover them all. And, as discussed above, there is no way to uniquely extract two dimensions of motion from a single vector measurement.

In this Section we consider the case in which horizontal motion is present but is ignored in the conversion from line-of-site to vertical motion. In this case, a non-zero horizontal velocity component will be interpreted as a vertical component. We can compute the vertical sensitivity to an unaccounted horizontal component in the following way. Once again, Equation 1 above, under the assumption that only vertical motion is present results in the following expression, Equation 3. Here, the argument of the cosine function corresponds to the geometry of both of the SAR systems used to date to acquire data for the Chino Basin Watermaster work. For other SAR systems, described in a separate section, that angle may be appreciably different.

$$d_v^{inferred} = \frac{d_t}{\cos(24)} \tag{3}$$

In the case that the $d_h=0$ assumption is made erroneously, then the error in the above expression will be given by:

$$d_v^{inferred} = d_v^{actual} - d_h^{actual}\tan(24) \tag{3}$$

The following figure shows the predicted error in the inferred vertical displacement in the case that the horizontal displacement is assumed to be zero, but is not. In this case, this plot shows the sensitivity of the

vertical measurement to the horizontal error. Note that this is generally not a random error but a systematic one associated with the presumably well-behaved horizontal motion. This result shows that an unaccounted horizontal error of 0.5 cm will be interpreted as a vertical displacement of 0.2 cm. As a result of this effect, a decision must be made regarding the interpretation of the data; assumptions regarding the presence of horizontal data may be made based on a physical model or another measurement type. Further, a more advanced implementation of InSAR is possible that is able to resolve motion into two directions – giving an additional capability to measure horizontal motion. This latter approach is discussed in the next section.

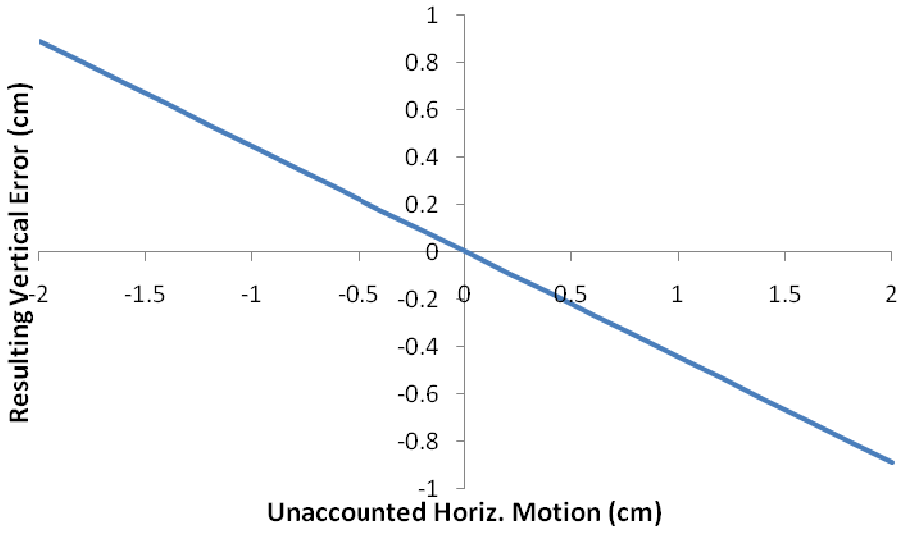

Figure 11: Predicted vertical error resulting from the assumption of no horizontal motion, in the case where horizontal motion is actually present. Note that the vertical error here is a bias, not a random error.

2.3.3. Opposite Side Interferometry (OSI)

In the conventional type of InSAR considered thus far, the satellite is, for each acquisition, in nominally the same position. Since the specific orbits considered here nearly cross the Earth's poles, this means that, the satellite is either east of the area of interest, looking west, or west of the area of interest looking east. The graphic in Figure 12 shows the orbit configuration for all the candidate satellite systems for Chino Basin imaging. Referring to Figure 12, the white lines indicate the direction of satellite travel. The satellite always images while "looking" to the right, but can operate while traveling north-to-south (descending) *or* south-to-north (ascending). The resulting imaged regions are shown (in color) for the corresponding orbit orientations.

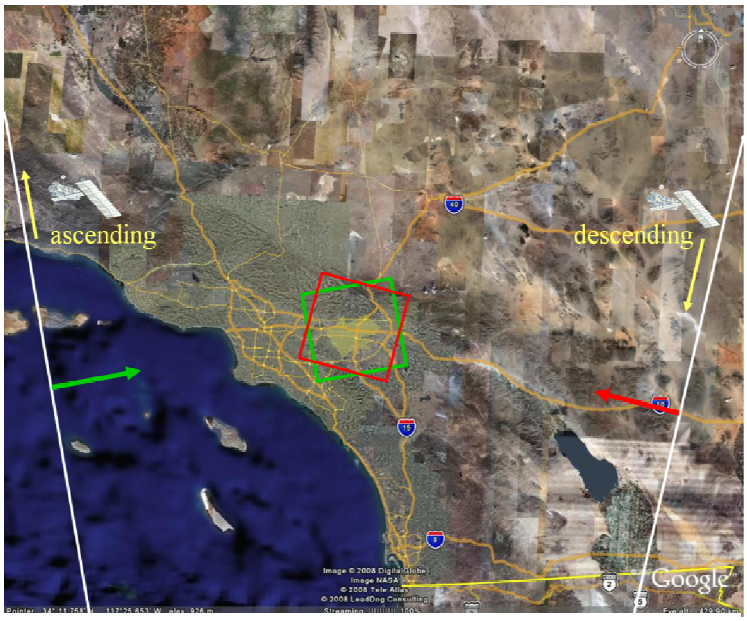

Figure 12: Ascending and descending orbits, both *looking* to the right, and the corresponding ground patches.

Referring back to Figure 3 this means that, depending on whether we are acquiring data from the ascending direction or from the descending direction, our LOS will be different (24 degrees to the left or to the right of the local normal.) Note that we cannot perform InSAR between an ascending and a descending pair. However, we *can* create a time series of InSAR ascending measurements and a time series of descending measurements over a similar time period, and combine these to resolve the vertical component and a horizontal component. This method has been applied in various tests over several years; the best documented result is that found in Hoffman[2] where it was determined that atmospheric interference at the particular region limited the measurement of horizontal motion to an accuracy of 1 to 2 cm. The behavior of the atmospheric interference in the Chino Basin *appears* to be more benign compared to that published in the journal article, but this is a qualitative assessment. Ascending and descending data from Chino Basin would have to be obtained (during the same time period) in order to demonstrate the ability of this technique for measuring the horizontal motion. There is an appropriate data set for this demonstration, which has been identified in the past. Without obtaining such a data set, for the particular area of interest, it is not possible to place a realistic bound on the potential performance of this technique. In addition, the data acquired during the 2008 Chino campaign using Envisat, appear to have resulted in excellent series for both the ascending and descending directions.

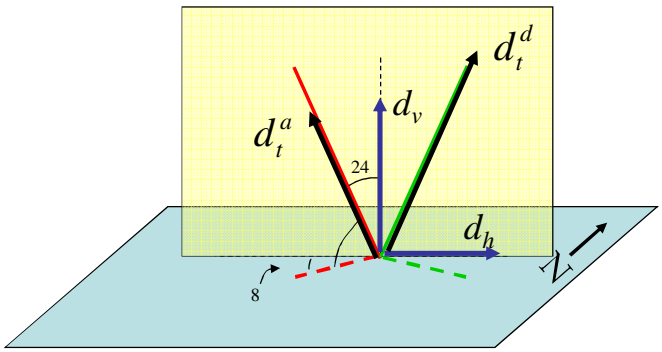

Figure 13: OSI geometry.

Based on the measured statistics of the Chino InSAR data presented above, we can estimate the expected horizontal motion error using the OSI technique. Figure 13 shows the relevant geometry. Assuming a model like that in Equation 1, we can write two equations describing the total displacement measured during the ascending pass and during the ascending pass. The expressions for the total displacements in terms of the vertical and horizontal (east-west) displacements are:

$$d_t^a = d_v \cos(24) + d_h \sin(24) \cos(8) \qquad (4)$$
$$d_t^d = d_v \cos(24) - d_h \sin(24) \cos(8)$$

Based on the two measurements d_t^a and d_t^d we can solve the above equations for the horizontal and vertical displacements. Since the standard deviations measured for the Chino InSAR data would apply to both the ascending and descending results, we can propagate the errors to computed displacement components (horizontal and vertical). Omitting the details of the error propagation, the results are shown in the following table:

Direction	Expression	St. Dev. (95%)
Horizontal	$\sigma_h = \frac{\sigma}{\sqrt{2}\sin(24)\cos(8)}$	1.22 cm
Vertical	$\sigma_v = \frac{\sigma}{\sqrt{2}\cos(24)}$	0.54 cm

[2] J. Hoffman and H. Zebker, Journal of Geophysical Research, V108, No. F1, 2003.

Note there has been a factor of $\sqrt{2}$ gain just by virtue of the fact that we are now using two data sets to estimate the components. The vertical error is now just over a half of a centimeter and the expected horizontal error is 1.22 cm. We consider this approach to be a good option for the Chino Basin, although a demonstration would be required using the recent 2008 data set.

2.4. Current SAR Sensors

The sensors we are considering in the historical and ongoing Chino monitoring, and in this analysis, consist of three European SAR systems that have been deployed beginning in the early 1990's. The table below summarizes relevant aspects of these systems. All sensors are C-band. The archive of SAR data begins with that acquired by the ESA ERS1 sensor following its deployment in 1991. Data for this sensor were collected by a satellite SAR with an exact repeat period of 35 days. With the exception of roughly a one year gap in this operation (when the satellite entered a different mode for ice monitoring) the archive is continuous and dense. In 1995 ESA launched a second C-band satellite (ERS2) which, for all intents and purposes, was identical to the first. This second satellite, initially in an orbit differing by only a single day, provides data that is fully coherent (in the interferometric sense) with ERS1. The archive for this second satellite extends to the present. However, due to hardware failures, useable interferometry data were acquired only through a portion of 2001.

Name/Country	Band	Best Res	Largest Swath	Years of Operation
ERS-1/ESA	C-band	25 m	100 km	1991-1998
RADARSAT-1	C-band	10 m	500 km	1994-
ERS-2/ESA	C-band	25 m	100 km	1995-
ENVISAT/ ESA	C-band Dual Pol	25 m	300 km	2002-

A third satellite launched by ESA in 2002, called ENVISAT, is also C-band. Unfortunately, due to some regulatory issues, the center frequency of this system was shifted slightly with the net result that ERS-ENVISAT interferometry is impossible except under very rare circumstances – it is certainly not operationally feasible. Nevertheless, this sensor provides a very good source of worldwide SAR data during the current decade. While a particular ENVISAT mode is virtually identical to the single ERS SAR mode, it also performs in a variety of other modes in which geometry and resolution are variable. However, the primary mode for this sensor is similar to that of ERS.

We include in this table a fourth system with performance similar to the other systems. In 1995, the Canadian Space Agency (CSA) launched a C-band SAR satellite that has been extremely successful and far outlived its design life. RADARSAT orbits in a slightly shorter repeat orbit, 24 days, and performs in a variety of modes. A primary discriminator of the RADARSAT system is the existence of a higher resolution mode (Fine Beam Mode) which delivers a ground measurement roughly 10m on a side. This mode is valuable for identifying features that are limited in spatial extent and can also be useful for noise limited situations. Another discriminator for this system is that data are considerably more expensive (by at least a factor of five) than for the other systems.

It is worthwhile to comment on the broader SAR environment – beyond the sensors used in the historical and ongoing Chino work. As has been discussed, the InSAR ground deformation effort to date has employed exclusively the data collected by the European Space Agency sensors ERS 1/2 and Envisat. For

the purposes of the work done to date, these are nominally the same systems with comparable capabilities. Clearly, the error calculations and measurements done here correspond to those systems. Other systems, of which there are at least a few, will possess different performance and different errors. In particular, the important parameters affecting error performance are radar frequency and system resolution. For the ERS and Envisat systems, the frequency is designated as C-band, which corresponds to a wavelength of 5.6 cm; and the "native" resolution of the system is about 5x20 m^2. The impact of each of these parameters is summarized below:

- Wavelength. SAR systems operate at a variety of wavelengths. Currently, the Japanese Space Agency operates a system (ALOS/PALSAR) at L-band, or a wavelength of about 24 centimeters. At the other end of the spectrum, the German space agency has recently launched a system, called TerraSAR-X that operates at X-band or about 3 cm wavelength. While other systems exist, or have existed, this represents the range of wavelengths available from current commercial data sources. The impact of wavelength on the types of errors considered here is complicated but the primary effect is in the sensitivity to atmospheric moisture. Since the higher frequencies interact more strongly with water vapor, these frequencies (smaller wavelengths) may exhibit stronger atmospheric signatures in the InSAR results. This has not been validated in a carefully controlled experiment, but it is the expectation. However, the situation is complicated by the fact that the higher frequencies (smaller wavelengths) are also more sensitive to ground motion. That is, a given surface motion distance will produce a larger response in a smaller wavelength system than in a longer wavelength system. There are competing effects and it is not clear which will dominate under various conditions. Finally, the higher frequencies (smaller wavelengths) will interact with vegetation more strongly and will produce a higher degree of decorrelation. Again, quantitative comparisons are underway but are highly dependent on the specific location. Nevertheless, one thing that is clear is the superior ability of the L-band radar to obtain measurements in areas of some vegetation. This is due to the ability of the longer wavelength radiation to penetrate vegetation that the shorter wavelength radiation cannot penetrate.
- Resolution. The new SAR systems are distinguished by a greater diversity in imaging modes that include polarimetry (not of general interest for displacement mapping), and high resolution modes. With resolutions as high as 3x3 m^2 these systems produce significantly greater detail than the previous generation. There are two potential contributions to the Chino monitoring effort that could be achieved with these new data sources. First, since the resolution determines the finest scale over which a motion feature can be measured, the higher resolution will lead to the measurement of smaller features, such as the displacement in the vicinity of an injection well, or the detail of the groundwater barrier. On the other hand, since the InSAR motion estimate is derived from the InSAR phase estimate, and since that phase estimate improves with the number of samples that comprise it, we can obtained improved estimates with higher resolution data simply by virtue of the larger number of samples of a given phase estimate at a given location. In the terminology of Section 2.1.1, we can reduce the decorrelation and therefore the uncertainty in the displacement estimate. In certain situations, this can be a considerable gain.

In Summary, the new SAR systems offer considerable improvement in SAR capabilities but do not necessarily offer great new opportunities for the Chino Basin monitoring program. Resolution is not a significant issue since the ground motion features of interest are many hundreds of meters in extent. The main area of potential contribution of the new systems is the ability of L-band radar to penetrate vegetation. This may allow access to some of the agricultural regions in the south part of the valley.

3. Leveling Overview and Error Sources

The practice of surveying encompasses a wide range of tools and techniques. Leveling has its roots in the 1800's and earlier but has evolved greatly to the present, taking advantage of precision materials, microprocessor technology and computer processing. The technique has well-established standards and practices, with an associated large literature and body of knowledge. Surveying now comprises a 4-year degree program at many universities. The breadth and depth of the field is considerable and is well beyond the scope of the work here. Primarily, we are interested in the errors present in surveying measurements. However, many techniques and types of equipment are used in the field. Strict standards exist for surveying practice but these do not necessarily translate directly into point-to-point measurement errors. As a result, it would be difficult to generalize a broad error analysis. In fact, such a generalization would not necessarily even productive for the purposes here. As we have done with the InSAR error analysis, instead of calculating the expected errors in the survey data, based on models of the environment, the equipment, and the collection procedure, we will use the measured data itself in order to focus on the errors associated with the specific area of interest. In particular, we seek to use the specific surveying data obtained for the Chino area. To this end, we have spent time with the surveying contractor for the Chino Basin, Associated Engineers, Inc. We were provided with particular data sets for one of the survey epochs, and from these data we are able to draw conclusions regarding accuracy – mostly based on the output of standard software and processing used by the company.

The approach used by Associated Engineers for both the vertical and horizontal surveys is a multi-node network run over several different routes. The vertical survey originates at the bench mark located at the Ayala Park extensometer. This technique takes advantage of redundant measurements across the network; the measurements are adjusted, based on a set of assumptions, in order to find the statistically optimal joint solution to the heights or separations of the intermediate bench marks. In what follows, we describe the process at a high level and present analysis of the output of the data processing in order to determine measurement uncertainties that can be presented in the context of the InSAR results above.

3.1. Leveling Survey

The vertical survey performed by Associated Engineers in Chino is comprised of a total of 53 miles and takes on the order of a week to perform. The procedure follows well established industry standards for this type of survey. The equipment type is considered to be appropriate for First Order leveling; the equipment is the Leica/Wild 3003 electronic level and invar rods. Extensive calibration of the equipment is done in accordance with, or exceeding industry standards. According to Jim Elliott, the Associated Engineers surveys fall within the expectation for the first order classification. This classification determines the permissible closure for the survey loops. The Class/Order of the survey generally are determined by the methods used and the equipment. For the surveys conducted here, the average turn length is about 125 feet with a maximum of 250 feet. These distances are sufficiently short that refractive effects of the atmosphere play virtually no role in the computation of the relative heights. Furthermore, atmospheric refraction as well as earth curvature effects are further reduced by the fact that turning points are always placed roughly midway between rod positions.

Measurements are acquired and electronically logged. Processing of the data is accomplished with an industry standard software package that implements an accepted statistical technique for data reduction and error propagation. The technique, Least Squares Adjustment, is well documented and a standard in the industry. An excellent reference on the subject (thanks, Jim Elliot) is [*Surveying Theory and Practice*, Robert E. Davis, et al., McGraw Hill, 1981]. The implementation of the algorithms here is in the form of a commercial software package, the STAR*LEV Adjustment Program, distributed by STARPLUS Software, Inc. This software has been used within the larger surveying community for over 20 years.

The primary output of the Least Squares Adjustment algorithm is the computed elevation for each bench mark, together with the computed statistics of the elevation estimate. It is the stated standard deviation for each of the points that contains the uncertainty in each of the measurements. As a result, following discussions with Marc Wilson (Associated Engineers), the software itself produces an output that characterizes the uncertainties in its computed quantities. That is, we can characterize the errors in the measured points based on the distribution of the standard deviation values produced by the software. Figure 14 contains a plot of the survey results as processed by the STAR*LEV program, for a particular Chino survey. This figure is the distribution of uncertainty values ascribed to each measured point. A total of 142 station occupations were included in this result of the fall 2007 survey. These standard deviations are shown here versus the number of occurrences of each. The analysis of such a distribution of distributions is unconventional but it is certainly straightforward to extract some meaningful results. I.e., the expectation (mean) value for this distribution is 0.48 centimeters. Slightly greater than 50% of the points correspond to a standard deviation value better than about 0.5 centimeters. It is also straightforward to show that 90% of the points have a standard deviation value of 0.71 cm or less. This means that the majority of the vertical measurements possess a 1-sigma uncertainty of this value (.71 cm) or less. In order to provide a fair comparison with the InSAR results presented above, and under the assumption that the original data follow a normal distribution, we can compute the 2-sigma deviation of the data. The mean 2-sigma deviation is .96 cm, and 90% of the points have a 2-sigma deviation of 1.42 cm.

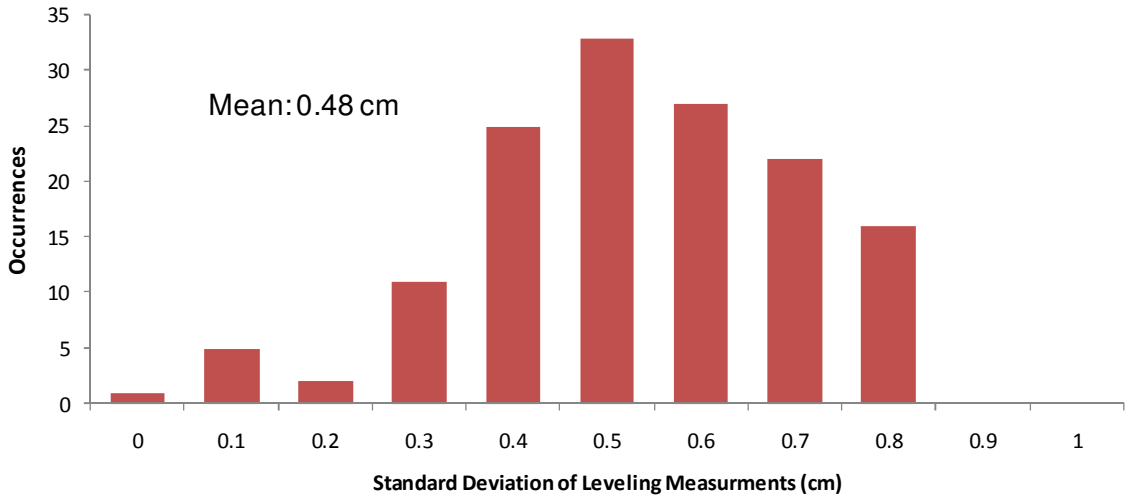

Figure 14: Distribution of two-sigma values for the Chino vertical survey from fall 2007. A total of 142 separate elevation values were used in the calculation of this figure.

3.2. Horizontal Survey

The measurement technology used for the horizontal survey is very different than that for the leveling survey, although the measurement methodology and processing are similar. The approach uses a two-frequency electronic distance measurement approach that provides accurate results over relatively long distances. The data acquisition proceeds by originating at a single fixed point and selecting a network to provide redundant measurements across the area of interest. Closure is achieved by returning to the starting point. The design of the horizontal network in Chino was driven largely by interest in the east-west component ground motion, especially associated with the fissure zone. As a result, the "strength" of the survey is significantly greater in the east-west direction than in the north-south direction. So much so that, in the following analysis, and based on discussions with AE, we only consider the east-west solution. In any case, data are processed using a least squares approach, which provides a horizontal position difference between bench marks, as well as the estimated error in that measurement. The software used by

Associated Engineers is the well-established, industry standard STAR*NET Adjustment Program. As was done for the vertical case, we turn to an actual data set from the City of Chino to represent the measurement errors. This particular data set was acquired during fall 2007. Horizontal data were acquired at a total of 42 stations. The diagram in Figure 15 shows the layout of the horizontal network. Note the density and continuity of the survey lines in the east-west directions – this is a visual indication of the strength of the survey in this direction.

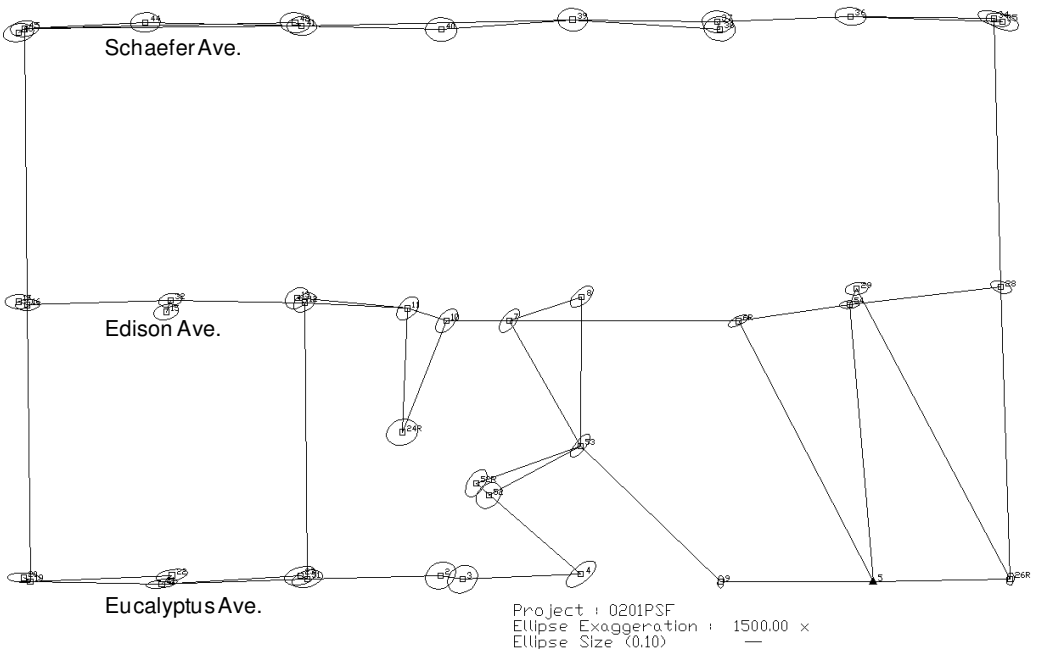

Figure 15: Diagram of horizontal survey points for the fall 2007 epoch. The survey is bounded by Monte Vista Ave. in the west and by Magnolia in the east.

An important point regarding the horizontal survey is that the main goal is to measure distance changes during each period, as opposed to changes in absolute position. The key challenge here is the fact that there is no local, reliable horizontal control. While it is possible to use horizontal control in the surrounding areas, an attempt to do so would be more costly and would be subject the accumulated errors associated with combining measurements over long distances. As a result, this survey was designed to use two points as local references. In the diagram in Figure 15, these references are located at the southeast and southwest corners. The southeast point is constrained in its northing and easting, while the southwest point is constrained in its northing. The presence of the fixed points in the vicinity of the measured motion suggests that the derived positions might be affected by motion of the reference points. This is especially the case of the absolute positional accuracy of the points, which is indicated in Figure 15 by the error ellipses centered on each measurement location.

The error ellipse is defined by the orthogonal axes of greatest and least uncertainty of the measurements. The graph in Figure 16 shows the distribution of the semi-major axis error values for the points in this horizontal survey. These points range to roughly 3.5 cm with the smaller values corresponding to the reference points at the lower left and right corners of Figure 15. However, once again, the absolute measurements are not the objective of this survey.

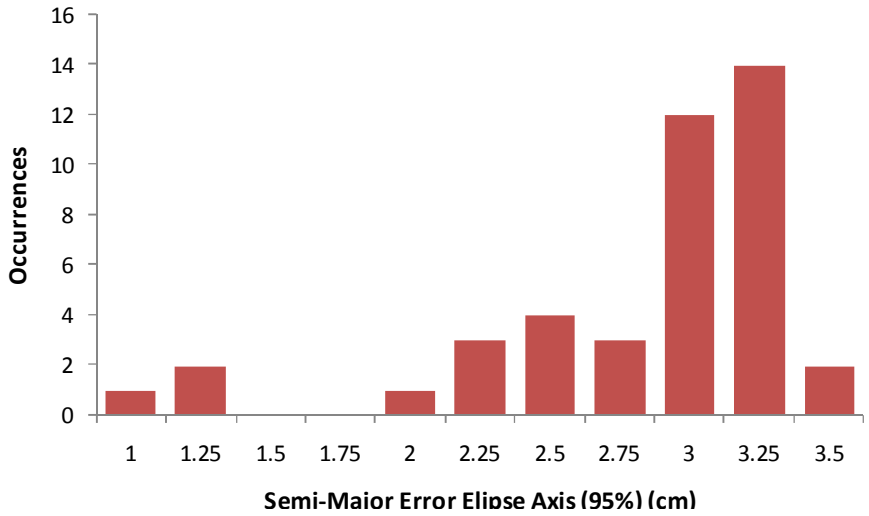

Figure 16: The distribution of the semi-major axis error values for the points in this horizontal survey.

In order to estimate the errors in the changes in the easting measurements, we can make use of the known characteristics of the equipment used as well as the geometry of the survey. It is possible to compute the standard error of the relative distance measurements analytically. This is valuable since the least squares process only provides error statistics for the absolute positions of the bench marks, not the relative positions. As a result, based on discussions with Jim Elliott, we use the theoretical error statistics, as computed *for this particular network*. Furthermore, since this survey is explicitly intended to support easting relative motion only, we limit the data used to those corresponding only to the east-west legs of the network shown in Figure 15.

For the particular equipment and survey of interest here these standard error results are shown in Figure 17. These 96 horizontal accuracy measurements represent the expected 2-sigma deviations for successive pairs of easting data. The computed mean for this survey is 1.10 cm. This is the value we ascribe to this process and, while there is not sufficient strength in the survey to derive an analogous metric to the northing component of the survey, we surmise that, given a symmetric survey, a comparable value would be obtained for both components. It is also important to recognize that the survey measurements are computed relative to a pair of possibly nonstationary reference points, under the assumption that they have not moved. In the case that either of these points *has* moved, then there will be a propagated error that impacts the measurements. Under this type of measurement scenario, it is critical that the reference points be located well outside of the areas of known or expected ground motion. The main issue here is the absence of horizontal control, which we address further in the conclusions and recommendations.

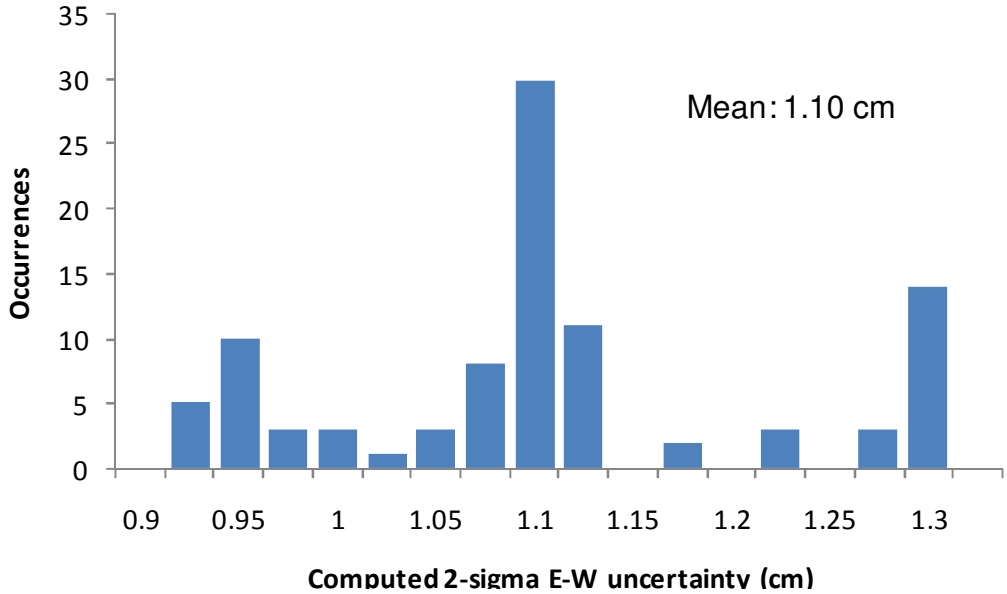

Figure 17: Distribution of standard error values for the particular survey and equipment used here.

4. Conclusions and Recommendations

The table shown on the following page summarizes the results of the analysis of InSAR and survey performance in the Chino area. For the vertical survey, there are several salient points. First, based on the analyses performed here, vertical errors in the InSAR approach are roughly half of those present in the leveling survey (assuming no horizontal motion). Furthermore, an important advantage of InSAR is the number and density of measurements available, roughly one measurement every 150 feet. This is compared to the current leveling surveys with measurements limited to discrete points separated by 1500 to 2500 feet. In addition, a single InSAR frame covers the entire Chino basin. This favors the InSAR technology from the standpoint of coverage, and possibly for identifying unknown signals that may be present over a wide area. However, the ability of leveling to make measurements at localized points is not necessarily a severe limitation so long the feature of interest is well defined and entirely covered by the survey. Depending on the location and phenomenology of interest, a potentially significant limitation of the InSAR data is that it measures, in the conventional application, the line-of-site component of the motion only. For the sensors used in the Chino area to date, the steep incidence angle (24 degrees) provides for roughly a 2 to 1 sensitivity to the vertical motion component relative to the horizontal component.

For the current approach to monitoring ground motion in the basin, a significant limitation is a lack of precise knowledge regarding the horizontal component of motion. For either of the measurement techniques, horizontal motion is not separable (conventional InSAR) or there is insufficient information to describe its accuracy (surveying). As has been discussed here, the approach to extracting the horizontal component from InSAR is very promising but not fully demonstrated. We revisit recommendations for OSI in a later paragraph. The horizontal survey is a well-demonstrated technique but, in this case, is not designed to fully exploit its potential. In particular, no horizontal control has been used so that difference measurements are impacted by the unknown horizontal motion of the reference points. Clearly, improved and better characterized measurements will require use of horizontal control in the area. There are two conceivable improvements to this network that may address this issue. The first is the possible use of existing horizontal control. Unfortunately, despite the existence of a large number of monuments in southern California, maintained by the NSF Plate Boundary Observatory (PBO), and the National Geodetic Survey's (NGS) continuously operating reference (COR) locations, only a single monument is in the vicinity of the region of interest. However, this is located approximately 2.8 miles from the Ayala Park extensometer.

On the other hand, a possible approach is to improve the horizontal survey by maintaining horizontal control using a GPS survey. Note that, while GPS is in principal a solution for the entire ground motion monitoring problem in the Chino area, in reality it will be severely limited by the presence of trees (obscuration of satellites) and power lines (interference and multipath). For these reasons, and based on discussions with Jim Elliott, a full GPS solution is not likely to be technically feasible. However a partial GPS solution remains feasible. A notional approach would be to use a network similar to that in Figure 15 with the end points of each horizontal leg provided by GPS coordinates obtained using survey grade GPS procedures and equipment. Such an approach should provide control for each leg with an accuracy of better than 1 cm, depending on the fidelity of the equipment and procedures. If it is desired, such a network could be expanded to provide improved strength in the north-south direction. Note that no consideration of cost has been factored in to this analysis.

	Comments	Error Analysis
	VERTICAL	
InSAR	The most common interpretation of the InSAR measurement is that it corresponds primarily to vertical motion. Under this assumption, we compiled data from 16 separate measurements over a common area (just NW of the main Chino subsidence feature). Based on roughly 15,000 pixels, we produced statistics for the error. • InSAR produces measurements (with the statistics quoted to the right) on a grid of roughly 150 feet. With newer satellite systems, this spacing may be improved. • Many 10's of square miles may be covered by a single data set – at intervals of roughly one month. • The conventional InSAR approach produces displacement measurements along the satellite line-of-site. These may be resolved to 2 dimensions using a priori knowledge. For data processed to date, sensitivity to vertical motion is 2x sensitivity to the horizontal component. • More advanced techniques may produce 2 dimensions of motion based on the data itself.	90% of the 2σ error values are 0.77 cm (0.025 ft) or less. Opposite-side-InSAR: 90% of the 2σ error values are 0.54 cm (0.018 ft) or less.
Survey	The industry standard STAR*LEV software produces statistics for each bench mark. These 1-sigma values are converted to 2-sigma (assuming Gaussian statistics). • The current Chino survey produces measurements at separations of roughly 1200 to 2500 feet over the extent of the main subsidence feature, with the Ayala Park extensometer used as reference. • Leveling provides explicit vertical measurements, independent of horizontal component. • Larger areas can be surveyed, although distance from Ayala Park extensometer results in measurement noise.	90% of the 2σ error values are 1.42 cm (0.047 ft) or less.
HORIZONTAL		
InSAR	As discussed above, conventional InSAR produces line-of-site displacements. We may assume horizontal-only motion (which is likely not of interest here), have *a priori* knowledge of vertical motion, or use the opposite side InSAR (OSI) approach to estimate the horizontal component. • Horizontal motion is not a typical direct output of conventional InSAR technique. Although, it can be done with *a priori* knowledge of vertical motion. • Opposite-side-InSAR (OSI) can produce separate horizontal/vertical components; requires twice the data. This technique has been demonstrated in a limited way. (Note that there is an excellent candidate Chino data set for this demonstration for 2008.)	Horizontal-only or *a priori* vertical: 90% of the 2σ error values are 1.73 cm (0.057 ft) or less. Opposite-side-InSAR: 90% of the 2-sigma error values are 1.22 cm (0.040 ft) or less.
Survey	The industry standard STAR*NET software provides standard errors computed based on the equipment characteristics and the geometry of the horizontal network. Since this survey is designed for easting strength only, only these values are analyzed. However, it is important to note that motion of the reference points, to the extent that it is present, will further degrade these values. • Predicted errors for horizontal difference survey are good but don't account for possible motion of reference points. • Survey is designed for superior strength in easting. • More stable horizontal control would improve results.	Easting 2σ error values are 1.10 cm (0.036 ft) or larger. Insufficient northing strength to estimate errors.

Finally, we return to the option of performing opposite side InSAR (OSI) at this site. Previous analysis (not for the Chino area) has been primarily limited by atmospheric interference. Our analysis presented above suggests a 2-sigma accuracy of 1.22 cm (easting) and 0.54 cm (vertical) or better. The procedure is sound and the main question regards whether the expected motion is sufficient to bring the horizontal signal above the noise. The basic approach of the publication referenced above is applicable in the general analysis of the data. In fact, the quality of the recent SAR data in the Chino area – for the period 2008 – is excellent and data have been acquired in both ascending and descending orbits. These data, not all of which have been purchased, exhibit excellent baselines for both ascending and descending passes. As a result, there is a good opportunity to demonstrate this technique assuming that there is sufficient motion during this period to provide a quality measurement above the noise. Based on the predicted noise levels, this would require a horizontal component on the order of 2 cm for this time period.

The current line-of-site InSAR approach to monitoring in the Chino basin area provides a high sensitivity to motion and, through the temporally dense data being acquired, sensitivity to its onset and time dependence. Although the conventional InSAR approach does not provide unique horizontal and vertical components, it certainly provides a measure of the magnitude of the motion to better than one centimeter. Collection of high quality data, with good baselines, has been very reliable for this frame. An excellent set of data, being processed as this report is being written, has been collected for 2008. The InSAR approach currently being pursued, in which many data acquisitions are being made and a dense subset is purchased, appears to be a very promising approach to capturing the dynamics of ground motion during the year. Furthermore, to the extent that the horizontal survey uses reference points that are well removed from the known subsidence regions, the technique should, based on the results below, provide measurements that are within about one centimeter. While a temporally dense set of data is usually preferable to a sparse one, the horizontal survey data can provide a pair of ground motion reference points for the InSAR survey, at spring and fall intervals. This continues to be valuable, especially in the case that significant motion is detected in the InSAR results. In that case, it should allow for separation of horizontal and vertical components, for the spring and fall measurements. According to the results here, more frequent horizontal surveys would provide additional insight into the horizontal/vertical motion components, but not necessarily any new information regarding the magnitude of motion or its onset.